Psychiatry Research: Neuroimaging 288 (2019) 1–11

Contents lists available at ScienceDirect

Psychiatry Research: Neuroimaging

journal homepage: www.elsevier.com/locate/psychresns

Circuit activity underlying a distinct modulator of prepulse inhibition

Linda Heidinger[a], James L. Reilly[a], Lei Wang[a,b], Morris B. Goldman[a,*]

[a] Department of Psychiatry, Northwestern University Feinberg School of Medicine, 446 East Ontario, Suite 7-100, Chicago, IL 60611, USA
[b] Department of Radiology, Northwestern University Feinberg School of Medicine, Chicago, IL, USA

ARTICLE INFO

Keywords:
Schizophrenia
Behavioral regressor
Attention
Functional MRI
Functional connectivity
Salience
Biomarker

ABSTRACT

Prepulse inhibition (PPI), the diminished eye blink response to a startling pulse induced by a prepulse, is regulated by brainstem, and modulated by cerebral, processes. Attentional modulation by the prepulse (AMP), a potential biomarker of psychotic disorders, differs from other modulatory processes because it only occurs if the interval between the prepulse and pulse exceeds 100 ms (>PP100). Videotaped eye blinks were measured during fMRI scanning in 15 healthy subjects hearing 64 pulse alone, 64 PP60 and 64 PP120 trials in a rapid event-related design. Because attentional influences on PPI vary spontaneously, we posited AMP could be isolated by comparing eye blink and Blood Oxygen Level Dependent covariation during the two PP trial types. Behavioral regressor coefficients reflecting significant covariation covered the insula and auditory cortices during PP120 but not PP60 trials. Clusters within the right anterior insula and auditory cortex were specific to AMP. Functional connections (FCs) between cerebral ROIs implicated in PPI were stronger during PP120 trials. The four FCs that were individually stronger during PP120 trials involved the right insula or auditory cortex and three were not present during PP60 trials. Converging evidence indicates the right insula is the hub of a network underlying AMP.

1. Introduction

Accumulating evidence indicates psychotic disorders are best conceptualized as disorders of neural circuit activity (Braff, 2015; Hyman, 2012). Core signs and symptoms arise from poorly characterized parallel and recursive circuits, however, greatly complicating efforts to isolate potential pathologic activity, distinguish this from compensatory activity, and determine its contribution to psychopathology (Logothetis, 2008). Fortunately, better characterized early sensory processing steps also appear relevant to the pathogenesis of psychotic disorders (Javitt, 2009; Swerdlow et al., 2008), can be linked to specific pathways and cognitive functions, and may also reveal discrete biomarkers and targets for future therapeutic interventions (Cuthbert and Insel, 2013; Fendt and Koch, 2013; Hyman, 2012).

1.1. Prepulse inhibition is a model of early sensory processing linked to psychotic disorders

Prepulse inhibition of startle (PPI) is a model of early sensory processing and one of the most widely utilized paradigms for studying the neurobiology and exploring potential therapies for psychotic disorders (Swerdlow et al., 2008; Fendt and Koch, 2013). The fundamental neural elements of PPI are present in all vertebrates and can be probed by two simple and discrete stimuli (Tabor et al., 2018). PPI in humans is typically defined as the diminished eye blink to a startling stimulus (pulse) induced by a preceding nonstartling stimulus (prepulse) (Graham, 1975) (Fig. 1). Converging evidence supports the view that the prepulse models a potentially relevant sensory stimulus, the startling pulse models a potent biologically-relevant distractor, and the diminished eye blink response models the CNS filtering of the distractor (Blumenthal et al., 2015). Despite its simplicity, PPI is correlated with human executive functioning (Bitsios et al., 2006; Scholes and Martin-Iverson, 2009); is blunted in psychotic disorders (Braff et al., 2001); can be normalized in animals models of schizophrenia by deep brain stimulation (Bikovsky et al., 2016) and is a valuable tool for identifying novel antipsychotic medications.

1.2. Passive paradigms identified cerebral modulation of PPI in animal models and humans

Brainstem pathways activated by the prepulse inhibit the startle response when the pulse follows about 30 to 250 ms after the prepulse (Fig. 1C: green arrows) (Fendt et al., 2001). These brainstem mediated effects are primarily determined by the intensity and duration of the

* Corresponding author.
E-mail address: m-goldman@northwestern.edu (M.B. Goldman).

https://doi.org/10.1016/j.pscychresns.2019.04.005
Received 31 May 2018; Received in revised form 1 January 2019; Accepted 15 April 2019
Available online 19 April 2019
0925-4927/

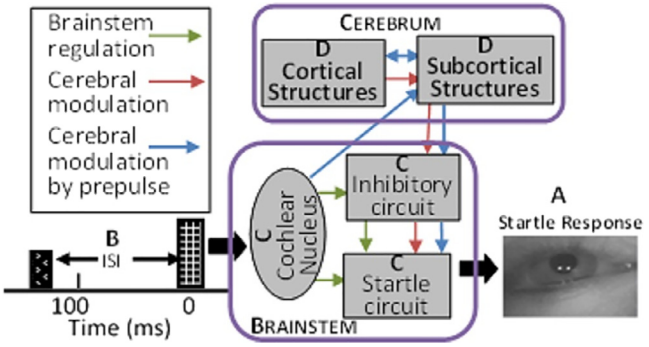

Fig. 1. Neural activity underlying AMP can be distinguished. Prepulse inhibition (PPI) of acoustic startle is the reduced startle response (A) to a startling stimulus (pulse) produced by a preceding nonstartling stimulus (prepulse) (B). The Figure illustrates a PP120 trial which contains a stimulus onset asynchrony (SOA) of 140 ms (interstimulus interval (ISI) of 120 ms). Separate brainstem pathways (C) activate and inhibit the startle response (green arrows). Processes within the brainstem mediate the impact of the intensity of the stimuli and the duration of the SOA on startle. These pathways also convey modulatory influences arising from cerebral processes (D) conveying, for example, the perceived salience of the stimuli, the subject's mood and general level of attentiveness (red arrows). Attentional modulation by the prepulse (AMP) differs from other cerebral influences because it is time-locked to trial onset and requires an SOA of at least about 100 ms in order to effect the eye blink response (blue arrows). Note that most of the imaged BOLD signal reflects neural activity generated after the eye blink response has occurred and at least some of this is likely proportional to the eye blink response. (For interpretation of the references to color in this figure legend, the reader is referred to the web version of this article.)

two stimuli as well as the time interval between them (prepulse/pulse interval (PP)). Swerdlow et al., 2001) demonstrated PPI was also modulated by activity originating in the cerebrum, in particular the prefrontal cortex, hippocampus, amygdala, striatum and thalamus (Fig. 1D: red arrows). These effects were demonstrated with 'passive' paradigms in which the significance of the PP trials and other cerebral processes that might influence PPI are not manipulated. His studies revealed that 'top-down' modulation by these structures involved neurotransmitters, and was responsive to pharmacologic treatments, implicated in psychotic disorders. Furthermore, functional imaging studies of Blood Oxygen Level Dependent (BOLD) activation utilizing passive paradigms substantiated the involvement of these cerebral structures in PPI in humans and identified differences in those with psychotic and other neuropsychiatric disorders (Table 1).

1.3. Active paradigms reveal more specific deficits

Subsequent studies also utilized 'active' paradigms which helped characterize cerebral modulatory effects related to stimulus novelty, complexity, and salience as well as the subject's mood, focus of attention, alertness and motivation (Filion and Poge, 2003; Roskam and Koch, 2006; Li et al., 2009). Active paradigms often involved more than one kind of prepulse. For instance, one of the means of studying the impact of attention on PPI was typically assessed using a selective attention task in which the subject was instructed to "count the low frequency prepulses and ignore the high frequency prepulses" (Schell et al., 2000). This paradigm revealed that making the prepulse (i.e. a potentially relevant stimulus) more relevant enhances PPI in normals but not in patients with psychotic disorders (Li et al., 2009). Further studies demonstrated that this blunted attentional influence on PPI in patients covaries more closely with deficits in higher cognition (Scholes and Martin-Iverson, 2010) and with severity of psychosis than PPI obtained with passive paradigms (Dawson et al., 1993, 2000; Hazlett et al., 2007). Other types of active paradigms (e.g. perceived spatial separation) also demonstrated the influence of attention to the prepulse (referred here as attentional modulation of PPI by the prepulse and abbreviated AMP) (Lei et al., 2018) and furthermore replicated the patient differences seen with the selective attention task (Yang et al., 2017). Functional imaging of AMP obtained with a selective attention task (Hazlett et al., 2008) demonstrated greater BOLD activity during the attend condition in bilateral striatum and thalamus and right middle frontal lobe in normals but not patients with schizophrenia (Table 1), consistent with the involvement of these structures in the AMP deficit. Together the findings suggested that AMP captures the entire PPI deficit in psychotic disorders (Scholes and Martin-Iverson, 2010) and that further characterization of the components of the underlying circuit could yield an objective, specific biological measure of the associated pathogenic processes (i.e. biomarker).

1.4. AMP can be distinguished from other cerebral modulators

Unlike other cerebral modulators of the startle response, AMP cannot take place until the prepulse-induced neural activity is conveyed from the brainstem to the cerebrum, processed within the cerebrum, and then conveyed back to the brainstem (Fig. 1C and D: blue arrows). In humans this takes about 100 ms (Ashare et al., 2007; Du et al., 2011; Li et al., 2009), and hence AMP cannot take place during trials with briefer PP intervals. Therefore trial-induced BOLD and eye blink responses that covary following trials where the PP interval is longer (e.g. PP120) but not shorter (e.g. PP60) than 100 ms may identify AMP. Indeed, this activity is likely to be specific to AMP since cerebral modulators of PPI unrelated to the current prepulse are independent of the PP interval and their influence will not covary with trial-induced BOLD responses. Indeed, the only other BOLD responses that might covary with concurrent eye blink responses in a passive paradigm would be a downstream consequence of PPI or startle. Unlike AMP, this activity should occur independently of PP interval.

1.5. Cerebral modulation of PPI varies spontaneously and can be seen with passive paradigms

One potential confound of using active paradigms to isolate AMP is they generate accessory cerebral processes also linked to trial onset that are specific to the attend task (e.g. 'count the low frequency prepulses') and hence introduce cerebral BOLD activity unrelated to AMP, per se. Rohleder et al., 2014, 2016) has shown in rodents, however, that an active paradigm is not necessary because of spontaneous variation in attention to the trial stimuli and the resulting startle response. In specific, they showed that prepulse- and pulse-induced neural activity was correlated with the propensity to exhibit PPI and startle across a range of rat breeds. In their first study, they demonstrated that neural activity associated with cerebral modulation of PPI is particularly prominent in the right pre-limbic cortex (the rodent analogue of lateral frontal lobes) (Rohelder et al., 2014). In the next study, they identified seeds in the left auditory cortex and right pre-limbic cortex where neural activity was highly predictive of PPI intensity, and demonstrated that activity in these seeds covaried with that in the anterior cingulate, insula, basolateral amygdala, and ventral hippocampus, i.e. many of the same cerebral structures associated with PPI in previous passive and active paradigms in both laboratory animals and humans (Table 1). Their analysis was facilitated by the showing that neural processes induced by the prepulse (e.g. PPI) produced activity negatively correlated with startle intensity while that induced by the pulse stimulus was positively correlated with the startle intensity.

1.6. Current study design and predicted findings

Based on the results of these studies we predicted we could isolate circuitry underlying AMP utilizing a passive paradigm by identifying where cerebral BOLD and eye blink responses covaried during PP120 but not PP60 trials. Based on Rohelder's et al. (2014, 2016)

Table 1
Cerebral structures where BOLD activity indicates an association with PPI during passive and active paradigms.

Study reference	Subjects	Paradigm/ Trial types[a]	Stimulus type/ Design[b]	PP > PA BOLD /Other methods[c]	Source/ Eye blinks and BOLD covary PP > PA[d]	Normals PP > patients PP BOLD/ Other
Kumari et al., 2003	Normals, Schizophrenia	**Passive**/ PP120, PA	Tactile/ Block	Striatum, thalamus, hippocampus, frontal & inf. parietal lobes	Outside/ Striatum, thalamus, inf. parietal lobe	Striatum, thalamus, hippocampus, frontal & inf. parietal lobes
Goldman et al., 2006	Normals	**Passive**/ PP120, PA	Auditory/ Rapid Event	None/ IRF L,R Insula; L,R auditory cortices	Outside/L,R insula	NA
Kumari et al., 2008	Normals, schizophrenia rx'ed with typical and atypicals	**Passive**/ PA, PP30, PP120	Tactile/ Block	Striatum, thalamus, hippocampus, insula, frontal & inf. parietal lobes	Outside/ L. thalamus	Thalamus, insula, frontal gyrus/Patients on atypicals intermediate with Normals
Campbell et al., 2007	Normals	**Passive**/ PA, PP120, PP480	Auditory/ Block	L,R striatum, R. ant cingulate	Outside/ L,R striatum, L,R thalamus, R,L cingulate, L inf. parietal lobe	NA
Neuner et al., 2010	Normals	**Passive**/ PA, PP140,	Tactile/ Rapid Event	R sup. parietal, R inf. frontal	Inside/ R striatum, L. med. frontal gyrus, R ant. cingulate	NA
Zebardast et al., 2013	Normals, Tourettes	**Passive**/ PA, PP100	Tactile/ Block	L, R sup. temporal, L, R insula, L,R Mid. Frontal, Inf. Parietal; L Ant., L Post. Cingulate	Inside/ L mid. frontal gyrus	R, L striatum; L inf. frontal; R. Ant. Insula; Post. Cingulate; L inf. parietal
Schulz-Juergensen et al., 2013	Normals, Enuresis	**Passive**/ PA, PP120; PP480	Auditory/ Rapid Event	None	Inside/ None	R,L Ant. Cingulate/ BOLD eye blink covary at PP120
Buse et al., 2016	Normals, Tourettes	**Passive**/ PA, PP120	Tactile/ Rapid Event	None reported	Inside/ none reported	Striatum, mid. frontal gyrus, cingulate, post central gyrus
Hazlett et al., 2001	Normals	**Active**/ PA, PP120	Auditory/ Event	Attend > Ignore: R,L thalamus	Outside/ none reported	NA
Hazlett et al., 2008	Normals, Schizophrenia, Schizotypal	**Active**/ PA, PP120	Auditory/ Event	Attend > Ignore: R, L striatum, R,L mid frontal lobe; R, L thalamus	Outside/ Left striatum	R,L striatum, R,L thalamus, R mid. frontal/ diminished attend effect in schizophrenia, intermediate In schizotypal

[a] 'Paradigm' refers to 'passive' (no subject instructions) or 'active' (subjects attend to some prepulses and ignore others) 'Trial type' PA refers to pulse alone trials; PP refers to prepulse followed pulse, the number is the interstimulus interval in ms.

[b] While PPI is traditionally assessed with auditory stimuli, PPI occurs with other sensory modalities and tactile stimuli are not degraded by scanner noise. Block designs provide a higher level of sensitivity but cannot determine individual trial-induced BOLD responses (nor their covariation with startle).

[c] 'PP > PA BOLD' identifies structures where BOLD activity was greater during PP than PA trials when assessed with a conventional voxel-wise ANOVA. Other methods refers to our paper where we relied on the timing and peak of the impulse response function (IRF) to identify PP-associated activity.

[d] 'Source' refers to whether eye blink responses were measured separately ('outside') or during ('inside') acquisition of fMRI scan. Unlike the current study, inside acquisition was obtained by EMG and scanner-induced artifact was modelled and subtracted from the EMG signal. Note Schulz-Jeurgesen could not demonstrate that either startle or PPI occurred in the scanner using an auditory stimulus, likely because of a degraded pulse (105 dB vs. >115 dB in this and others using auditory stimuli) or complexity of the gradient artifact. While most studies did not measure eye blinks in the scanner, one can assume PPI occurred because they typically utilized louder prepulses and pulses or tactile stimuli which are not degraded by the scanner noise.

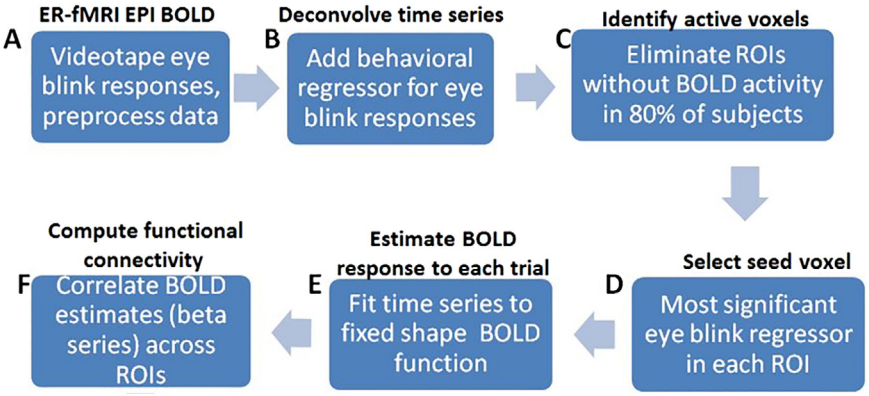

Fig. 2. Analysis of circuit activity underlying attentional modulation of PPI by the prepulse (AMP). A: 64 PA, 64 PP60 and 64 PP120 trials were administered over four runs in an event-related design while eye blink responses were videotaped. B: Ratings of the intensity of eye blink responses were incorporated into the GLM to estimate the extent variations from the mean BOLD response covaried with eye blink responses for each trial type for each voxel (BR coefficient). C: To identify functional connections (FCs) associated with covarying BOLD/eye blink responses we first limited ourselves to active voxels in preselected ROIs where at least 80% of subjects demonstrated BOLD activity. D: The voxel in each of these ROIs with the most significant BR coefficient for each trial type served as the seed for the FC. E: The magnitude of the BOLD response to each trial was estimated for each seed. F: Functional connection strengths for each trial type were estimated by correlating the magnitudes across seeds. See Methods section for further details.

observations, we also predicted that the sign of the covariation between BOLD and eye blink responses for PPI in general and AMP in specific would be negative. We utilized the previous human BOLD imaging studies to pre-select cerebral regions of interest (Table 1, Supplemental Figure 1). In our previous study we had found BOLD activity in the auditory cortices and the anterior insula to be potentially associated with AMP (Goldman et al., 2006; Table 1), and thus predicted these structures would constitute part of the AMP circuitry.

2. Methods

2.1. Participants

Forty-eight healthy volunteers between the ages of 18 and 35 (27 males, 21 females) were recruited and provided informed written consent to a protocol approved by the IRB at Northwestern University, Chicago, IL. Selection criteria and PPI screening were previously described (Goldman et al., 2006). In brief, all subjects could detect 40 dB tones in the ranges of 250 to 6000 Hz and had no history of a neurologic disorder or a personal or family history of mental illness. PPI was measured in a mock scanner during 24 randomly presented trials containing pulse alone (white noise, 104 dB for 40 ms) (PA); prepulse (white noise, 88 dB for 20 ms) followed 60 ms later by pulse (PP60ms) or prepulse followed 120 ms later by pulse (PP120) trials. Eye blink responses to the 24 trials were measured with electromyography. Responses in millivolts were recorded every ms for 250 ms after the onset of the pulse stimulus. Waveforms were rectified and filtered below 100 and above 300 Hz. Peak startle amplitudes were determined if a) the average amplitude of the 20 ms baseline did not exceed 5 mv; b) the onset, defined as an increase of at least 3 mv above the mean of the trailing 4 samples, occurred in the first 20 to 120 ms of the recording and c) the peak occurred within 150 ms. To enhance detection of covarying BOLD and eye blink responses in the MRI scanner we only included those 18 subjects exhibiting >50% PPI. This was done because previous studies which compared eye blink and BOLD responses to PA and PP140 trials had limited ability to detect activity specific to the prepulse (Neuner et al., 2010; Table 1) which was central to our study aims. Two of the eighteen subjects could not be scheduled and one was excluded due to scanner malfunction leaving a final sample of 15.

2.2. fMRI data acquisition and pre-processing

Images were acquired at the Northwestern University Center for Translational Imaging on a Siemens 3T TIM Trio whole body magnet equipped with a 12-channel head coil. Thirty-two interleaved 3.0 mm slice EPI BOLD axial oblique functional slices (T_2*-weighted, 2000 ms TR, 20 ms time of echo (TE), 77° flip angle, fat saturation, field of view (FOV) 206 × 220, matrix size 120 × 128) were obtained during four 10 min runs. The first 6 images were discarded leaving 288 images covering the whole brain for each run. Onset of startling pulses occurred 140 ms after the onset of a TR (i.e. the pulses were lined up across trials). Between the second and third runs, a 10-min structural MRI scan was obtained using a 1 mm isotropic MPRAGE with the following scanning parameters: TR/TE = 230 ms/2.9 ms, flip angle 9°, TI = 900 ms, matrix of 256 × 256, FOV = 256 mm, slice thickness = 1 mm, no gap, covering the entire head left to right using 176 slices.

2.3. Stimulus presentation and eye blink recording in the scanner

During the MRI scan, subjects heard 192 trials in pseudo-randomized order at 8–16 s (mean 12 sec) jittered intervals. The 64 trials of each trial type contained the same stimuli used in the mock scanner, except the intensity of the pulse was adjusted to 117 dB to overcome scanner noise. Stimuli were generated by a Human Startle Response Monitoring System (SRLAB, San Diego Instruments, San Diego, CA) amplified with a Sony STR DE 185 amplifier before being played through JBL 2425 h/j speakers (Stamford, CT, USA) placed in a custom-designed speaker box. 1¼″ wide polyethylene air conduction tubing led through a wave guide into padded MRI compatible headphones (Scan Sound Inc. Coral Springs, FL, USA).

2.4. fMRI data and eye blink processing

Sequential analytic steps are summarized in Fig. 2. Eye blink responses were captured every 17 ms from the right eye with an infrared emitter and camera (MRA Inc. Washington, PA, USA), then converted to a digital signal (Canopus 110 ADVC, San Jose, CA, USA) and analyzed with Vegus Studio 10.0 software (Fig. 2A). Blinks were rated only if their onset was after frame one following the pulse (17 ms) and before frame 7 (119 ms), and the peak occurred before frame nine (153 ms). Each blink was rated on a seven-point scale from no response to sustained eye closure over two consecutive frames (Essex et al., 2003) (Table S1). Inter-rater reliability of 0.84 was demonstrated. Essex et al., 2003) previously demonstrated a high correlation between EMG and video-taped measures in 31 subjects (mean $r = 0.84$). We also measured eye blink intensity in an additional seven subjects and found a mean $r = 0.74$ (range 0.50 to 0.97). fMRI data pre-processing and initial analyses were conducted with Analysis of Functional NeuroImages (AFNI) software (Cox, 1996; Goldman et al., 2006). The general linear model (GLM) included 42 regressors: 12 modeling constant, linear and quadratic variability in the baseline BOLD signal over each run; 21 modeling the hemodynamic response at trial onset and the subsequent six TRs for each trial type; 6 modeling rotational and translational

Table 2
Demographics; startle response, PPI and SCM across trial types.

	Value (±SD)			Statistics (2-tailed *P*)	
Subjects (*n*)[a]	15			–	
Age (years)	24.2 ± 3.8			–	
Gender	Male	Female			
	8	7		>0.50	
Startleintensity[b]	PA	PP60	PP120	PA vs PP	PP60 vs PP120
	4.8 ± 1.3	3.9 ± 1.6	3.1 ± 1.6	**0.0001**	**0.0001**
PPI (%)	PP60	PP120			
In Scanner	20.4 ± 16.0	35.4 ± 20.8		<**0.003**	
Mock Scanner	43.0 ± 28.3	85.2 ± 10.9		<**0.001**	
Stimulus correlated motion (SCM)[c]	PA	PP60	PP120	PA vs PP	PP60 vs PP120
Translational (mm)	.015 + 0.024	.017 + 0.026	.018 + 0.029	*0.07*	0.87
Motion Outliers (%)	0.23 + 0.31	0.13 + 0.16	0.24 + 0.21	0.25	**0.04**

[a] Two subjects were Asian, one Hispanic, one African-American and the remainder Caucasian. Two were smokers and they were not instructed to refrain from smoking on the day of the study. All subjects were right-handed.
[b] Mean eye blink intensity rated with Essex criteria following videotaping in the scanner.
[c] Mean SCM motion was minimal. Translational motion was marginally greater during the two prepulse pulse (PP) than the pulse alone (PA) trial types and motion outliers were significantly greater during PP120 than PP60 trials.

subject motion and 3 behavioral regressors (BRs) which reflected the covariance of eye blink and BOLD responses for each trial type (Neuner et al., 2010; Wood et al., 2008). The BRs were computed by first replicating the stimulus timing file and replacing the values denoting trial onset with the rated eye blink response; then files were convolved with a gamma-variate function representing the ideal HDR for a 12 s BOLD response; next, the resulting vectors were standardized and finally orthogonalized to the stimulus convolution matrices of the impulse response functions (IRFs) of all three trial types as well as to each other (Buchel et al., 1998). Thus, for each voxel in each subject, the GLM analysis yielded a 12-s long IRF modeling the mean hemodynamic response and a BR coefficient estimating the correlation of the variation from this mean to the variation from the mean eye blink response on a trial by trial basis for each trial type (Fig. 2B).

2.5. Subject-level ROI and functional connectivity analysis for each trial type

ROIs for the connectivity analysis were restricted to 22 pre-selected cerebral structures linked in previous imaging studies to PPI (Table 1, Figure S1). After transforming each subject's data to Talairach space, ROI borders were delineated from the San Antonio Talairach Daemon (Lancaster et al., 2000). Active voxels within these ROIs were defined applying a false discovery rate (FDR) of $q < 0.2$ to the partial F-stats of the IRF to help assure only voxels exhibiting BOLD responses were considered for seed selection while at the same time minimizing false negatives (Genovese et al., 2002). Type I error was controlled by limiting the connectivity analysis to those preselected ROIs in which at least 80% of subjects exhibited activity for at least one trial type (Richter et al., 2013) (Fig. 2C). The active voxel in each of these qualifying ROIs that exhibited the most statistically significant BR coefficient was selected as the seed (Jennings et al., 1998; Stein et al., 2000) (Fig. 2D). The BOLD response to each of the 64 trials in each seed was estimated by correlating a fixed shape gamma variate function with the BOLD signal at the onset and the six TRs following each trial (beta-series correlation, AFNI 'Individual Modulation') (Fig. 2E) (Rissman et al., 2004). Finally, the strengths of the functional connections (FCs) were estimated by correlating these 64 beta coefficients between the qualifying ROI pairs (Fig. 2F) (Cisler et al., 2014).

2.6. Statistical analyses

Data for the three trial types were transformed into two Helmert contrasts (H1, H2). H1 reflects differences between PA and the two PP trial types and H2 reflects differences between the two PP trial types. Mean translational motion between trial onset and the subsequent TR, computed from the three translational regressors, and the number of BOLD outliers/image volume occurring during the TR following trial presentation (Whitfield-Gabrieli et al., 2009) were relied on to estimate stimulus-correlated motion. Stimulus-correlated motion confounds data analysis (Johnstone et al., 2006) though this is somewhat mitigated by event-related designs. (Morgan et al., 2007)

To facilitate comparison with previous studies (Table S1), a conventional voxel-wise group-level mixed effects ANOVA was performed on the mean of the 2nd, 3rd and 4th regression coefficients of the IRF (Goldman et al., 2006). An analogous assessment of the BR coefficients identified clusters where the covariance of BOLD and eye blink responses differed between the two PP trial types. Subsequent ROI-based analyses were conducted using subject-level mixed effects hierarchical linear regression (Goldman et al., 2006; Hedeker and Gibbons, 1996). Subject was the level three random effect, ROI or ROI pair the level two random effect, and the outcome measure for each trial type was the level one factor (e.g. Z-transformed BR regressor coefficient, number of active voxels, Z-transformed correlation coefficient).

3. Results

Table 2 contains the subjects' demographic characteristics, mean eye blink responses and indices of stimulus correlated motion. Consistent with normal habituation, eye blink intensity diminished about 25% over the four scanner runs (Figure S2). The drop was proportional across trial types, however, and percent prepulse inhibition ($PPI = (1 - (PP_{60/120}/PA)) \times 100$) thus remained constant. Mean PPI in the scanner, based on videotaped eye blink responses, was diminished relative to ($t = 5.6$, $df = 4$, $P < 0.001$), but highly correlated with ($r = 0.67$, $df = 45$, $P < 0.0001$), that obtained with EMG. Consistent with the literature, startle intensity was about 25% greater during pulse alone than PP60 trials, which, in turn, was about 25% greater than PP120 trials (Braff et al., 2001). Eye blink intensity was included as a covariate in the subject-level analyses to help assess if differences in startle/PPI intensity accounted for trial type differences in BOLD activity. Both of the indices of stimulus correlated motion differed across trial types, but this movement appeared to be minimal and the indices were unrelated to each other or to startle intensity. In any case, these were also included as covariates in the subject-level analyses.

3.1. Group level voxel-wise ANOVA confirms pulse masks prepulse–induced BOLD

The conjunction analysis of BOLD responses yielded 13 clusters

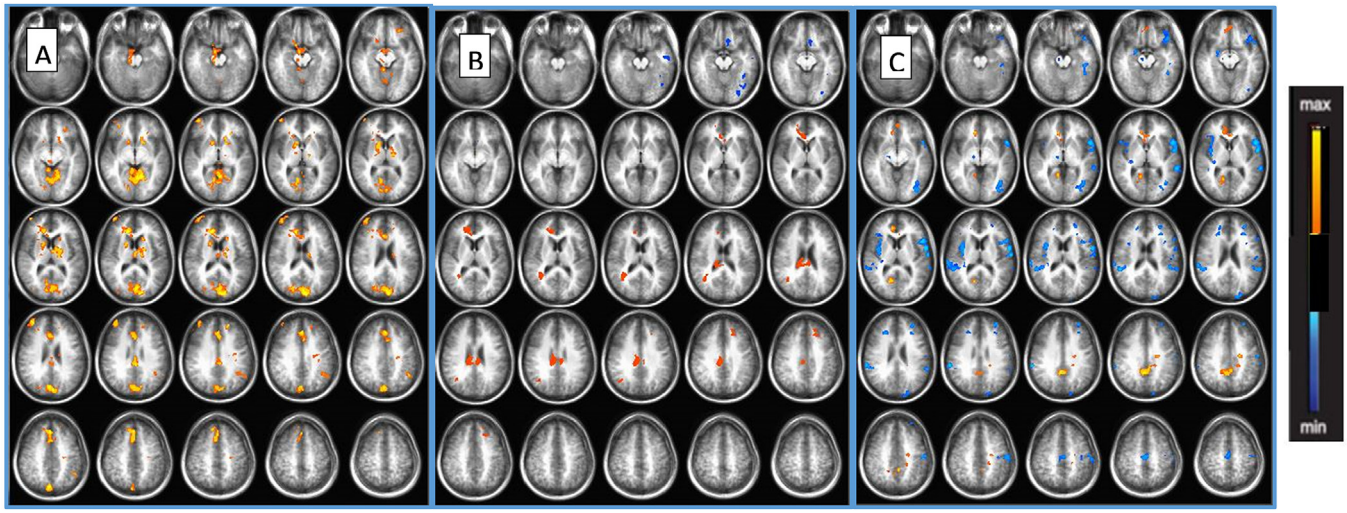

Fig. 3. BR coefficients estimate unique association between BOLD and eye blink responses for each trial type. Voxels exhibiting positive (yellow-red) or negatively-signed (blue) correlations between BOLD and eye blink responses were mapped using a liberal threshold ($P < 0.05$, uncorrected; linear smoothing) for A) Pulse alone (PA), B) PP60 and C) PP120 trials. Note differences between trial types are accentuated by orthogonalizing the BR vectors to each other because it largely eliminates activity in one trial type if it is completely swamped by identical activity found in another trial type. The relative ratio of positive to negative coefficients across voxels substantiates the visual impression that negatively signed voxels predominate during PP120, relative to PP60, trials in: whole brain (ratio 2:1 (positive/negative) for PP60 trials, 1:3 for PP120 trials (H2: $P < 0.00001$)); preselected ROIs (PP60 5:1, PP120 1:3, H2: $P < 0.000001$); and the insula (H2: $Z = 2.6$, $P < 0.01$), but no other, preselected ROIs. (For interpretation of the references to color in this figure legend, the reader is referred to the web version of this article.)

(Table S2A; Figure S3) which overlapped the structures identified in previous imaging studies (Table 1). The Helmert contrast comparing pulse alone (PA) to the two PP trial types (H1) yielded five clusters all showing greater BOLD responses during PA trials (Table S2B; Figure S4). The contrast comparing PP60 to PP120 trials (H2) yielded one cluster showing a greater response during PP60 trials (Table S2C; Figure S5). Thus, the conventional voxel-wise ANOVA resembled the comparable analysis in our previous study (Goldman et al., 2006) which showed pulse-induced BOLD responses (e.g. startle) swamped prepulse-induced responses (e.g. PPI). Thus unlike other investigators listed in Table 1 we could not use this analysis to identify BOLD activity specific to either PPI or AMP.

3.2. BR coefficients distinguish between pulse- and prepulse-induced neural activities

BR coefficients quantify covarying BOLD and eye blink responses and hence provide a more direct indication of neural activity associated with startle modification. Pulse alone (PA) trials generated dispersed and prominent positive BR coefficients throughout the CNS (Fig. 3A); PP60 trials generated a scattering of inconspicuous positive coefficients as well as some negative coefficients in the left inferior cortices (Fig. 3B); while PP120 trials generated some prominent positive coefficients within the medial prefrontal cortex, posterior cingulate and precuneus as well as bilateral bands of negative coefficients covering the insula, auditory and parietal cortices and scattered areas in the left inferior cortices (Fig. 3C). The sign of the coefficients appeared analogous to that described by Rohelder et al. (2014, 2016) who also found that neural activity was positively correlated with pulse-induced (i.e. startle) and negatively correlated with prepulse-induced (i.e. PPI) responses. Hence, we treated negative BR coefficients as potentially indicative of PPI or AMP. The ratio of positive/negative coefficients differed significantly between the two PP trial types (Legend, Fig. 3), and comparison of the pattern in the two PP trials suggested that activity in the left inferior cortices seen with both trail types was a consequence of PPI and the bands of negative BR coefficients exclusive to the PP120 trials were consistent with AMP though they conceivably reflect the greater PPI during the PP120 trials. The source of the prominent positive coefficients in the medial prefrontal cortex, posterior cingulate and precuneus during PP120 trail was unclear, but could reflect the protective effects of AMP on activity with the default mode network which overlaps these structures.

3.3. ANOVA of BR coefficients link AMP to right insula and right 2° auditory cortex

A group level ANOVA identified nine clusters where BR coefficients differed between the two PP trial types. BR coefficients in all nine were more negative during PP120 trials (Table 2, Fig. 4), and thus could represent either activity attributable to greater startle during PP60 trials, greater PPI during PP120 trials or AMP. Clusters #2 (right auditory cortex and inferior parietal lobule) and #7 (right anterior insula) are clearly indicative of AMP since 1) they overlap areas where prominent bands of negative coefficients are apparent during PP120 trials (Fig. 3C), but 2) where neither positive nor negative BR coefficients are apparent during PP60 trials (Fig. 3B), and 3) the PP60 BR coefficients are consistently positive (Table 3, last three columns) and thus unlikely to reflect lower levels of PPI. Clusters 1, 4, 6, 9 are suggestive of AMP in so far as PP120 BR coefficients are consistently negative while PP60 BR coefficients are consistently positive (2 SD below 0) (Table 3, last three columns), though none overlap the negative bands in Fig. 3C.

3.4. Active voxels and functional connections implicate same structures in AMP

To constrain type 1 error, seed selection for the functional connections was limited to voxels demonstrating active BOLD responses ('active voxels') (Fig. 2C). The number of active voxels was positively correlated with the startle response regardless of trial type (Table 4, next to last column), consistent with the conventional voxel-wise ANOVA of BOLD activity indicating that pulse-induced generally swamped prepulse-induced BOLD activity (Table S2). The only exceptions were the insula and auditory cortices consistent with the assessment of the BR coefficients (Fig. 3, Table 3) and our previous study (Goldman et al., 2006).

To further constrain type I error, the circuit analysis was limited to the nine ROIs in which nearly all (>80%) subjects exhibited some voxel activity (Fig. 2C; Table 4, last column). The active voxel in the resulting

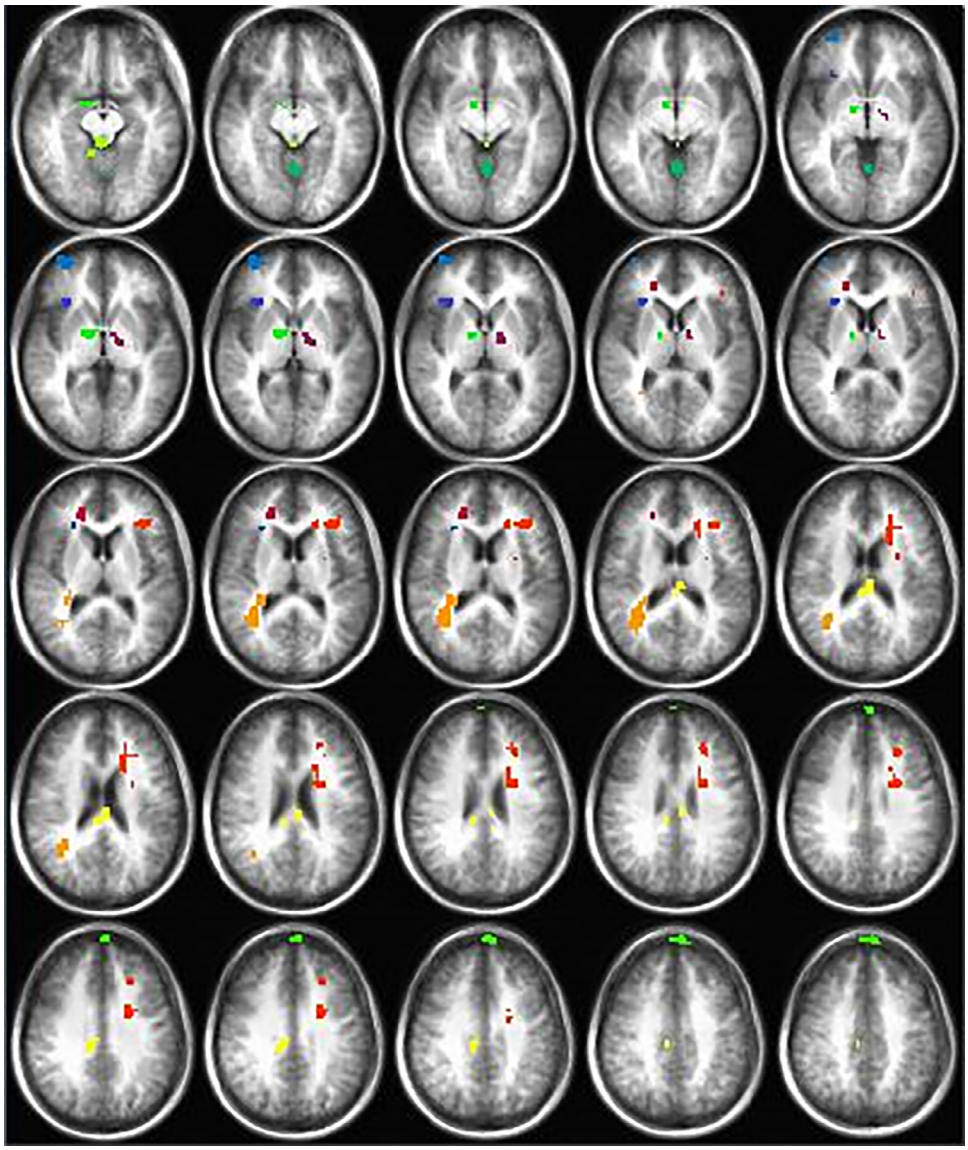

Fig. 4. Clusters where BR coefficients differ during PP60 and PP120 trials. Note the left side of images are the right side of subjects. See Table 2 for additional cluster information. red = left cingulate, insula, caudate; orange = right angular gyrus, 2° auditory cortex; yellow = posterior cingulate; light green = right superior frontal gyrus; green = right thalamus; light blue = right middle frontal gyrus; dark blue = right anterior insula; purple = left thalamus; dark red = right anterior cingulate. Note two clusters were not in the cerebrum: yellow green = cerebellar vermis; blue green = culmen; brainstem. (For interpretation of the references to color in this figure legend, the reader is referred to the web version of this article.)

Table 3
Differences in the sign and magnitude of cerebral behavioral regressor coefficients for the two PP trial types[a].

Cluster #	Vox-els	Peak Voxel			Nearest Gray Matter	Color[b]	BR Coefficients (mean + SD)[c]		
		X	*Y*	*Z*			PP60	PP120	*Student*[d]
1	137	−19	13	23	L. Insula, middle frontal lobe, caudate	Red orange	0.59 ± 0.22	−0.37± 0.22	−71
2	79	34	−49	17	R. 2° auditory cortex, inferior parietal	Orange	0.69 ± 0.25	−0.31±0.16	−46
3	52	−4	−25	23	Posterior cingulate	Yellow	0.87 ± 0.35	0.02 ± 0.22	−21
4	40	4	64	26	Superior frontal lobe	Pale green	0.78 ± 0.39	−0.39 ± 0.16	−26
5	33	10	−1	−9	R. thalamus	Green	0.65 ± 0.23	−0.22 ± 0.19	−37
6	29	34	58	2	Right middle frontal lobe	Light blue	0.53 ± 0.29	−0.44 ± 0.22	−31
7	28	28	22	2	R. insula	Dark Blue	0.76 ± 0.19	−0.31 ± 0.16	−31
8	25	−13	−7	5	L. thalamus	Purple	1.31 ± 0.34	−0.14 ± 0.14	−17
9	25	19	37	14	R. anterior cingulate	Dark red	0.65 ± 0.18	−0.34 ± 0.22	−35

[a] Threshold and cluster size: $P < 0.04$ for 25 or more adjacent voxels (uncorrected).

[b] Colors correspond to map in Fig. 4.

[c] Mean (±SD) BR coefficients reflect the extent that variations from the mean HDR response in each cluster voxel correlate with variations from the mean eye blink response for that trial type. Mean PP120 coefficients were significantly more negative than PP60 coefficients in all nine clusters but this in itself does not identify AMP. All but clusters 3, 5, 8 are consistent with AMP, while these three likely reflect greater startle seen with PP60 trials, since PP60 BR coefficients are consistently positive (2 SD > 0) while PP120 coefficients do not differ from 0.

[d] Paired *t*-test of BR coefficients for PP60 and PP120 trials across voxels. The large *t* values reflect the consistency of the differences in BR coefficients across each voxel in a given cluster.

Table 4
Subjects with voxel activity; mean active voxels (± SD) and correlation with eye blink intensity in preselected ROIs[a].

Region of interest		Left PA	Left PP60	Left PP120	Right PA	Right PP 60	Right PP 120	Active voxels vs eye blink r, (P)[c]	Activity in at least 80% of subjects[b]
Nucleus accumbens	**Active voxels***	29 + 92	2 ± 7	0.3 ± 1	31 + 96	34 + 88	1 ± 2	0.221 **(0.036)**	Neither side
	Subjects (n)	3	3	2	6	5	4		
Anterior cingulate	**Active voxels**	33 + 90	24 + 79	2 ± 9	37 + 94	32 + 85	1 ± 3	0.263 **(0.012)**	Neither side
	Subjects (n)	5	4	1	6	4	1		
1° Auditory (BA41)	**Active voxels**	44 + 15	43 + 16	45 + 14	51 + 13	45 + 21	53 + 22	0.016 (0.878)	**L**(eft), **R**(ight)
	Subjects (n)	15	15	15	15	15	15		
2° Auditory (BA42)	**Active voxels**	25 + 18	22 + 16	25 + 18	33 + 13	25 + 13	29 + 13	0.122 (0.252)	**L,R**
	Subjects (n)	13	14	14	15	14	14		
Caudate	**Active voxels**	24 + 46	21 ± 47	8 ± 14	24 + 43	24 + 45	6 ± 9	0.290 **(0.006)**	Neither
	Subjects (n)	10	7	5	10	7	4		
Hippocampus	**Active voxels**	3 ± 9	3 ± 8	0.3 ± 1	3 ± 9	3 ± 10	1 ± 1	0.282 **(0.007)**	Neither
	Subjects (n)	3	3	3	4	3	3		
Insula	**Active voxels**	176 + 150	139 + 138	134 + 109	175 + 136	134 + 193	143 + 114	0.197 (0.078)	**L,R**
	Subjects (n)	15	14	15	13	15	15		
Globus pallidus/ Putamen	**Active voxels**	59 + 143	42 + 85	7 ± 22	47 + 72	30 + 74	12 + 36	.335 **0.001**)	Neither
	Subjects (n)	9	7	5	8	6	5		
Middle frontal	**Active voxels**	76 + 175	60 + 181	34 + 81	97 + 204	90 + 204	38 + 91	0.227 **(0.032)**	Neither
	Subjects (n)	6	7	5	10	7	7		
Parahippo-campus	Active Voxels	46 + 72	38 + 61	9 ± 21	32 ± 53	30 + 68	5 ± 10	.327 **(0.002)**	**L**
	Subjects (n)	13	11	5	10	11	7		
Thalamus	**Active voxels**	114 + 165	87 + 155	23 + 41	91 + 88	61 + 75	32 + 48	.300 (**0.004**)	**L,R**
	Subjects (n)	13	12	8	12	11	7		

[a] The first row shows the mean (+/- SD) number of active voxels for each hemisphere of the ROI during each trial type. Active voxels defined by false discovery rate ($q = 0.2$) primarily to minimize false negatives. The second row shows the number of subjects with at least one active voxel for that trial type.

[b] To further diminish the risk of type I error we limited the functional circuit analysis to those ROIs where at least 80% of the subjects ($n = 12$) had active voxels for at least one of the trial types.

[c] Mean correlation between number of active voxels and mean eye blink response for each trial type across subjects. Significant correlations indicate voxel activity is proportional to, and thus potentially attributable to, startle intensity (recall PA trials do not induce PPI). Only in the insula and auditory cortices is it clear that BOLD activity cannot be attributed to startle intensity, and only in the right insula and left 2° auditory cortex do more subjects exhibited voxel activity during PP than PA trials.

Table 5
Differences in the BR coefficients of seed voxels[a].

Region of Interest	*Statistics (two-tailed P)*[b] *PA vs PP (H1)*	*PP60 vs 120 (H2)*	*Hemi-sphere*	*Hemi*H1*	*Hemi*H2*
1° Auditory ((BA41))	0.52	0.31	0.89	0.62	0.37
2°Auditory (BA42)	0.93	*0.09*	0.58	0.74	0.29
Insula[c]	0.40	**0.009**	0.42	0.39	0.54
Parahippocampus	0.11	0.21	–	–	–
Thalamus[c]	**0.008**	0.37	0.82	0.79	0.83

[a] The Table displays the statistical significance of the difference in BR coefficients for seed voxels in the nine ROIs that qualified for the circuit analysis. Note none of the findings appeared to be lateralized.

[b] *P* values reflect mixed model linear regressions (Subject level 2, *t* stat level 1).

[c] Accounting for differences in eye blink intensity could not account for differences between the PP trial types in the insula (adjusted H2; $Z = 2.51$, $P = 0.012$), consistent with evidence in the text that insular BR coefficients reflect AMP. In contrast, accounting for eye blink intensity nearly eliminated the differences between PP and PA trials in the thalamus (adjusted H1: $Z = 2.01$, $P = 0.044$) indicating differences were largely attributable to differences in startle intensity.

nine ROIs which contained the most significant BR coefficient served as the seed for the connectivity analysis, thereby linking the functional connectivity analysis directly to startle modification (Table 5). BR coefficients in the PP120 insula seeds appeared specific to AMP since they were more negative than the PP60 seeds and the difference could not be attributed to differences in eye blink responses (i.e. PPI or startle) (Table 5, Legend). The mean of the 36 correlation coefficients, reflecting the strength of the cerebral functional connections (FCs), was greater during PP120 (0.41 ± 0.22) than PP60 trials (0.35 ± 0.24, H2: $Z = 2.98$, $P = 0.003$) which, in turn, resembled PA trials (0.36 ± 0.24) (Fig. 2D and E; Table S3). 12 of the 36 connections were not significant during the PP60 trials whereas only four were not significant during PP120 trials ($\chi^2 = 5.1$, $P = 0.02$). These differences also could not be attributed to differences in eye blink responses (analysis with eye blink response as covariate: H2: $Z = 3.65$, $P = 0.0002$).

Subject-level mixed effects hierarchical linear regression analysis identified four of the 36 FCs that were each stronger during PP120 trials (Table 6). Three of these involved the right insula and two involved the right 2° auditory cortex. The other two ROIs that made up the circuit were the right and left thalamus (Figure S6). Three of these four FCs were not significant during PP60 trials (Table 6, Legend), and the strength of one covaried with PPI across subjects only during PP120 trials as could only occur with AMP (Table 6, last column).

4. Discussion

4.1. A novel methodologic approach isolates a single component of PPI

This is the first study to identify the functional circuitry underlying a discrete cerebral influence, attentional modulation by the prepulse (AMP), on prepulse inhibition (PPI) in humans. AMP was distinguishable because it was both time-locked to trial onset and only took place if the time interval between the prepulse and pulse exceeded about 100 ms (Fig. 1). Hence, BOLD and eye blink responses that covaried during otherwise identical trials that exceeded (i.e. PP120), but not during those that were shorter (i.e. PP60) than, 100 ms localized AMP. The distinction between pulse- (i.e. startle) and prepulse- (i.e. PPI) induced neural activity was greatly facilitated by the fact that the former

Table 6
Functional connections strengths differing by trial type[a].

	Correlation (SD)			Statistics		
ROI pair	PA	PP60	PP120	PA vs PP(H1) *Z, P*	PP60 vs 120 (H2) *Z,P*	H2*mean eye blink intensity *Z,P*
R Insula - R 2° Auditory	0.44 ± 0.25	0.45 ± 0.22	0.58 ± 0.19	−1.27,*0.20*	−2.11,***0.03***	1.16, *0.24*
R Insula - R Thalamus	0.25 ± 0.26	0.17 ± 0.23[b]	0.28 ± 0.14	0.43,*0.66*	−2.25,***0.02***	0.18, *0.86*
R Insula - L Thalamus	0.26 ± 0.23	0.19 ± 0.18[b]	0.34 ± 0.14	1.23,*0.29*	−2.56,***0.01***	1.42, 0.15
L Thalamus-R 2° Auditory	0.22 ± 0.21	0.20 ± 0.14[b]	0.35 ± 0.16	−0.91,*0.36*	−2.33,***0.02***	−2.59, ***0.001***[c]
R Thalamus -L Thalamus	0.50 ± 0.19	0.51 + 0.17	0.29 ± 0.14	2.08, ***0.04***	2.68,***0.01***	1.82,0.07
L 1° Auditory-R1° Auditory	0.54 ± 0.18	0.39 ± 0.29	0.45 ± 0.22	2.20,***0.03***	−0.92,*0.35*	0.98,*0.32*

[a] 36 functional connections (FCs) between the nine retained ROIs were generated for each trial type by correlating the 64 beta estimates of the BOLD response from that trial type's seed voxel with those in the other ROIs of that trial type. The Table shows the six FCs that differed significantly. Note the first four functional connections are stronger for PP120 than PP60 trials, and the last two are stronger for PA than the two PP trials. Table S3 shows statistical differences for all 36 FCs.

[b] Three of the four FCs that were stronger during PP120 than PP60 trials did not appear to even exist during the PP60 trials (i.e. $r < 0.24$). Table S3 identifies other FCs that were not significant for each trial type.

[c] Eye blink intensity and its interaction with trial type were added to assess whether PPI predicted connection strength more for PP120 trials as might be expected with AMP. The interaction was significant for the L Thalamus - R 2° Auditory connection reflecting that this FC strength covaried with mean PPI during PP120 but not PP60 trials. None of the H1 *eye blink interactions were significant (not shown).

were consistently positively-correlated and the latter negatively-correlated with eye blink activity (Fig. 3, Table 3). The circuitry underlying AMP was assessed by comparing PP120 and PP60 functional connection strengths between seeds whose BOLD and eye blink covariation were most significant across cerebral ROI pairs previously associated with PPI (Figure S1;Table 1) (and hence most likely to reflect circuit activity associated with PPI) (Fig. 2). These functional connection strengths were determined by estimating the BOLD response to each trial of the given type and correlating these estimates across ROI pairs. Those seed pairs in ROIs that appeared both specific to AMP and whose functional connections were stronger during PP120 trials, and particularly if they did not exist during PP60 trials, identified AMP circuit elements.

4.2. AMP centered in circuit emanating from right insula

Functional cerebral connections between all ROI pairs were both more plentiful and more pronounced during the PP120 than PP60 trials (Table S3), consistent with a dispersed cerebral circuit specific to AMP. The series of analyses converged on the right insula as the hub of this functional circuit (Figures S6). Thus, 1) large bands of activity of covarying BOLD and eye blink responses indicative of PPI (i.e. negative BR coefficients) covered the bilateral insula, auditory and parietal cortices during the PP120 (Fig. 3C) but not the PP60 (Fig. 3B) trials; 2) a cluster of voxels in the right insula and in the right auditory cortex/inferior parietal lobe appeared specific to AMP while clusters in several other cerebral structures were highly suggestive of it (Table 3, Legend); 3) furthermore, PP120 voxels that constituted the seed for the insula circuit elements also appeared specific to AMP (Table 5); and 4) three of the four individual functional connections that were stronger during the PP120 trials involved the right insula and only one of these was apparent during the PP60 trials (Table 6). Finally, the findings replicated those of our previous study (Table 1) and closely matched our predicted findings.

4.3. Alternative interpretations can be excluded

These findings cannot be attributed to the greater PPI apparent during PP120 than PP60 trials (Table 2) because accounting for this only made the previously noted difference between PP120 and PP60 ROI pairs more significant and did not eliminate the finding linking PP120 insula seeds to AMP (Table 5). Indeed, PP60 trials induced minimal evidence of cerebral activity closely associated with PPI (i.e. BR coefficients) (Fig. 3B), and in fact covarying PP60 BOLD and eye-blink activity in all nine cerebral clusters appeared to reflect pulse (i.e. startle: positive BR coefficients) effects (Table 3, last three columns). Other modulatory influences on PPI cannot be responsible because they are not time locked to trial onset and hence their impact on PPI would not covary with trial-induced BOLD responses. Differences in pulse-induced activity are also not responsible since the pulse clearly generated positively signed BR coefficients (Fig. 3A), while the findings in question were all negatively signed (Fig. 3C, Tables 3 and 5), and because the key structures in the AMP circuit (insula and auditory cortices) were the only ROIs where pulse induced activity could not account for PP120 eye blink responses (Table 4, Legend). Other cerebral processes cannot be invoked because we used a passive event-related paradigm and thus any other process should have been randomized across trial types. Stimulus correlated motion (Table 1) can be excluded because it was minimal (Table 1), unrelated to startle intensity, and was accounted for in the statistical analyses. Finally, chance seems highly unlikely not only because of the multiple steps taken to diminish type I error but because of the consistency of the results across different outcome measures.

4.4. Consistency with results reported by other investigators

While there are significant differences in study design that limit the ability to compare this study to the previous work of others, our findings are consistent with the literature. The original animal studies with passive paradigms also implicated cortical-thalamic-striatal structures in PPI (Swerdlow et al., 2001; Rohelder et al., 2016); while an active paradigm of attentional modulation also implicated the auditory cortex (Du et al., 2011) and a passive paradigm of cerebral modulation also implicated the right prefrontal cortex, insula and anterior cingulate (Rohleder et al., 2014, 2016). The previous human BOLD imaging studies with passive paradigms also reported findings in striatum, thalamus, anterior cingulate, inferior parietal lobe and frontal cortex (Table 1) consistent with both our map of BR coefficients (Fig. 3) and our cluster analysis (Table 3). Given its prominence in the current and our previous study, we cannot, however, offer a compelling explanation for why the insula was not consistently linked to PPI in most of the previous imaging studies. The previous studies which directly assessed AMP with an active paradigm (Hazlett et al., 2001, 2008) (Table 1) also reported findings in the thalamus and prefrontal cortex (Table 3), though they found striatal involvement which exceeded that apparent in our study (Fig. 3C). Their reported absence of activity in the insula, in contrast, may simply be attributable to the fact that they did not look there.

4.5. Significance of functional circuit to psychotic disorders

The findings are consistent with the view that the reduced AMP in psychotic disorders arises from the impaired salience detection that is

found in psychotic disorders. The insula, and particularly the right anterior insula contribute to salience detection (Cauda et al., 2012) and its component processes (i.e. sustained attention (Dosenbach et al., 2007) and auditory processing (Bamiou et al., 2003)). Bilateral thalamus involvement is also critical to this network (Liang et al., 2013). Impaired salience detection in psychotic disorders has been associated with dysfunction of the insula and specifically altered connectivity of the anterior insula (Goodkind et al., 2015; Palaniyappan et al., 2013; Walter et al., 2016; Wylie and Tregellas, 2010).

4.6. Limitations of study design and interpretation

Several issues limit interpretation of these findings. First, the sample size was small, composed only of young adults, and limited to those exhibiting at least 50% PPI. Hence, additional work with larger samples that are more representative of the general population are needed, particularly when patients are to be assessed. Furthermore, multiple comparisons were not rigorously controlled, though this was mitigated by other steps to limit type I error and the overall consistency of the various outcome measures (Fig. 2). AMP was inferred using a passive paradigm that eliminated potential confounds and enhanced the power of the design, but did not directly manipulate AMP. Hence it is important findings are replicated using an active paradigm (e.g. Hazlett et al., 2008) that directs the subjects' attention to and from the prepulse. Other factors limit the precision of the results, such as the fact that functional connectivity is correlative, does not address causality and may not reflect anatomical connections; ROIs were defined in common rather than in individual neurological space; pulse and prepulse intensity were not modified to preserve functionally equivalent effects as is commonly done in electrophysiology and psychophysics; and seeds for the circuit analysis were selected on BR coefficient significance of a single voxel.

4.7. Conclusions and future directions

Psychotic disorders appear to arise from dysfunction of distributed neural networks, but deconstructing these networks, linking the elements to cognitive functions, targeting disordered activity and distinguishing it from adaptive/compensatory activity is a daunting task (Fox, 2018). Because AMP reflects a single contribution to a quantifiable and interpretable evolutionarily-preserved cognitive process specifically linked to chronic psychosis, findings like those reported here may offer a more expedient route to enhance diagnosis and treatment of psychoses.

Deep brain stimulation may normalize PPI deficits in obsessive compulsive disorder (Kohl et al., 2015), and transcranial magnetic stimulation offers a non-invasive means of testing if a non-invasive stimulus can normalize AMP and associated cognitive deficits in psychotic disorders (Etkin, 2018). TMS applied to surface nodes of cerebral networks appear to enhance activity and function of the entire network (Downar et al., 2016; Hallett, 2007; Wang et al., 2014). In particular, TMS applied to the right middle frontal lobe appears to enhance insular connectivity (Gratton et al., 2013) and augment putative insular-mediated therapy (e.g. smoking cessation) (Li et al., 2017). The right middle frontal lobe is a key component of the salience network and associated with both PPI and AMP (Hazlett et al., 2008); a cluster in this ROI located on the cerebral surface (Fig. 4) appeared closely associated to AMP (Cluster #6, Table 2); and was highly connected with the right insula during PP120 but not PP60 trials (data not shown). TMS effects on insular circuit activity, PPI and putative cognitive functions that are limited to PP120 trials would provide compelling evidence of the circuit's involvement in AMP and could lead to novel therapeutic treatments for psychotic disorders.

Acknowledgments

The authors wish to acknowledge the contributions of William Bieth; Brandon Gardner, MD, PhD; Fozia Ghafoor, MD;, PhD; Kirti Kulkarni MD; Sarah Lia Nainggolan MD; Robert Lyons; Donald G. McLaren, PhD; Stephanie Papillon MD; Nicholas Patniyot, MD; Luiz Pessoa PhD; Todd Parrish PhD; Matthew Schroeder PhD; Steve Small, MD, PhD; Mathew Smith, Ph.D. Anna Solodkin PhD; Tommi Raij, MD. PhD.; Xue Wang PhD; Zuoli Zhang, MD; and the staffs of the University of Chicago and Northwestern University imaging centers for this work. Many of the above individuals made sustained and/or essential contributions to the development and success of the study design as well as data collection and analyses. Much of the intellectual backbone of this study was also provided by those listed above. Funding provided by the Brain Research Foundation of the University of Chicago and a NARSAD Independent Investigators Award to MBG. The authors declare they have no conflicts of interest.

Contributors

All authors contributed to the writing and revisions of the manuscript. Ms. Heidinger is an image analyst and she developed or modified many of the analytic approaches used to characterize the BR coefficients and the functional connectivity, as well as interpret this data. Dr. Reilly is a neuropsychologist and helped with the design of the study and interpretation of the data. Dr. Wang develops multimodal image biomarkers and he provided guidance for all aspects of the study. Dr. Goldman developed the major ideas that lead to the study and oversaw all aspects of its completion. None of the authors have a conflict of interest relevant to this publication.

Supplementary materials

Supplementary material associated with this article can be found, in the online version, at doi:10.1016/j.pscychresns.2019.04.005.

References

Ashare, R.L., Hawk Jr., L.W., Mazzullo, R.J., 2007. Motivated attention: incentive effects on attentional modification of prepulse inhibition. Psychophysiology 44, 839–845.
Bamiou, D.E., Musiek, F.E., Luxon, L.M., 2003. The insula (Island of Reil) and its role in auditory processing. Brain Res. Rev. 42, 143–154.
Bitsios, P., Giakoumaki, S.G., Theou, K., Frangou, S., 2006. Increased prepulse inhibition of the acoustic startle response is associated with better strategy formation and execution times in healthy males. Neuropsychologia 44, 2494–2499.
Bikovsky, L., Hadar, R., Soto-Montenegro, M.L., Klein, J., Weiner, I., Desco, M., et al., 2016. Deep brain stimulation improves behavior and modulates neural circuits in a rodent model of schizophrenia. Exp. Neurol. 283, 142–150.
Blumenthal, T.D., Reynolds, J.Z., Spence, T.E., 2015. Support for the interruption and protection hypotheses of prepulse inhibition of startle: evidence from a modified attention network test. Psychophysiology 52, 397–406.
Braff, D.L., 2015. The importance of endophenotypes in schizophrenia research. Schizophren. Res. 163, 1–8.
Braff, D.L., Geyer, M.A., Swerdlow, N.R., 2001. Human studies of prepulse inhibition of startle: normal subjects, patient groups, and pharmacological studies. Psychopharmacology (Berl) 156, 234–258.
Buchel, C., Holmes, A.P., Rees, G., Friston, K.J., 1998. Characterizing stimulus-response functions using nonlinear regressors in parametric fMRI experiments. NeuroImage 8, 140–148.
Buse, J., Beste, C., Herrmann, E., Roessner, V., 2016. Neural correlates of altered sensorimotor gating in boys with tourette syndrome: A combined EMG/fMRI study. World J. Biol. Psychiatry 17, 187–197.
Campbell, L.E., Hughes, M., Budd, T.W., Cooper, G., Fulham, W.R., Karayanidis, F., et al., 2007. Primary and secondary neural networks of auditory prepulse inhibition: a functional magnetic resonance imaging study of sensorimotor gating of the human acoustic startle response. Eur. J. Neurosci. 26, 2327–2333.
Cauda, F., Costa, T., Torta, D.M., Sacco, K., D'Agata, F., Duca, S., et al., 2012. Meta-analytic clustering of the insular cortex: characterizing the meta-analytic connectivity of the insula when involved in active tasks. NeuroImage 62, 343–355.
Cisler, J.M., Bush, K., Steele, J.S., 2014. A comparison of statistical methods for detecting context-modulated functional connectivity in fMRI. NeuroImage 84, 1042–1052.
Cox, R.W., 1996. AFNI: software for analysis and visualization of functional magnetic resonance neuroimages. Comp. Biomed. Res. 29, 162–173.
Cuthbert, B.N., Insel, T.R., 2013. Toward the future of psychiatric diagnosis: the seven

pillars of RDoC. BMC Med 11, 126.
Dawson, M.E., Hazlett, E.A., Filion, D.L., Nuechterlein, K.H., Schell, A.M., 1993. Attention and schizophrenia: impaired modulation of the startle reflex. J Abnorm. Psychol. 102, 633–641.
Dawson, M.E., Schell, A.M., Hazlett, E.A., Nuechterlein, K.H., Filion, D.L., 2000. On the clinical and cognitive meaning of impaired sensorimotor gating in schizophrenia. Psych. Res. 96, 187–197.
Dosenbach, N.U., Fair, D.A., Miezin, F.M., Cohen, A.L., Wenger, K.K., Dosenbach, et al., 2007. Distinct brain networks for adaptive and stable task control in humans. Proc. Natl. Acad. Sci. USA 104, 11073–11078.
Downar, J., Blumberger, D.M., Daskalakis, Z.J., 2016. The neural crossroads of psychiatric illness: an emerging target for brain stimulation. Trends Cogn. Sci. 20, 107–120.
Du, Y., Wu, X., Li, L., 2011. Differentially organized top-down modulation of prepulse inhibition of startle. J. Neurosci. 31, 13644–13653.
Essex, M.J., Goldsmith, H.H., Smider, N.A., Dolski, I., Sutton, S.K., Davidson, R.J., 2003. Comparison of video- and EMG-based evaluations of the magnitude of children's emotion-modulated startle response. Behav. Res. Methods Instrum. Comput. 35, 590–598.
Etkin, A., 2018. Addressing the causality gap in human psychiatric neuroscience. JAMA Psychiatry 75, 3–4.
Fendt, M., Li, L., Yeomans, J., 2001. Brain stem circuits mediating prepulse inhibition of the startle reflex. Psychopharmacol. 156, 216–224.
Fendt, M., Koch, M., 2013. Translational value of startle modulations. Cell Tissue Res. 354, 287–295.
Filion, D.L., Poje, A.B., 2003. Selective and nonselective attention effects on prepulse inhibition of startle: a comparison of task and no-task protocols. Biol. Psychol. 64, 283–296.
Fox, M.D., 2018. Localizing symptoms to brain networks using the human connectome. NEJM 2237–2245.
Genovese, C.R., Lazar, N.A., Nichols, T., 2002. Thresholding of statistical maps in functional neuroimaging using the false discovery rate. NeuroImage 15, 870–878.
Goldman, M.B., Heidinger, L., Kulkarni, K., Zhu, D.C., Chien, A., McLaren, et al., 2006. Changes in the amplitude and timing of the hemodynamic response associated with prepulse inhibition of acoustic startle. NeuroImage 32, 1375–1384.
Goodkind, M., Eickhoff, S.B., Oathes, D.J., Jiang, Y., Chang, A., Jones-Hagata, L.B., et al., 2015. Identification of a common neurobiological substrate for mental illness. JAMA Psychiatry 72, 305–315.
Graham, F.K., 1975. Presidential address, 1974. The more or less startling effects of weak prestimulation. Psychophysiology 12, 238–248.
Gratton, C., Lee, T.G., Nomura, E.M., D'Esposito, M., 2013. The effect of theta-burst TMS on cognitive control networks measured with resting state fMRI. Syst. Neurosci. 7, 124.
Hallett, M., 2007. Transcranial magnetic stimulation: a primer. Neuron 55, 187–199.
Hazlett, E.A., Buchsbaum, M.S., Tang, C.Y., Fleischman, M.B., Wei, T.C., Byne, W., et al., 2001. Thalamic activation during an attention-to-prepulse startle modification paradigm: a functional MRI study. Biol. Pscyh. 50, 281–291.
Hazlett, E.A., Dawson, M.E., Schell, A.M., Nuechterlein, K.H., 2008. Probing attentional dysfunctions in schizophrenia: startle modification during a continuous performance test. Psychophysiology 45, 632–642.
Hazlett, E.A., Romero, M.J., Haznedar, M.M., New, A.S., Goldstein, K.E., Newmark, et al., 2007. Deficient attentional modulation of startle eyeblink is associated with symptom severity in the schizophrenia spectrum. Schizoph. Res. 93, 288–295.
Hedeker, D., Gibbons, R.D., 1996. MIXREG: a computer program for mixed-effects regression analysis with autocorrelated errors. Comput. Methods Programs Biomed. 49, 229–252.
Hyman, S.E., 2012. Revolution stalled. Science translational medicine 4, 155cm111.
Javitt, D.C., 2009. Sensory processing in schizophrenia: neither simple nor intact. Schizophren. Bull. 35, 1059–1064.
Jennings, J.M., McIntosh, A.R., Kapur, S., 1998. Mapping neural interactivity onto regional activity: an analysis of semantic processing and response mode interactions. NeuroImage 7, 244–254.
Johnstone, T., Ores Walsh, K.S., Greischar, L.L., Alexander, A.L., Fox, A.S., Davidson, R.J., et al., 2006. Motion correction and the use of motion covariates in multiple-subject fMRI analysis. Hum. Brain Mapp. 27, 779–788.
Kohl, S., Gruendler, T., Huys, D., Sildatke, E., Dembek, T.A., Hellmich, M., et al., 2015. Effects of deep brain stimulation on prepulse inhibition in obsessive-compulsive disorder. Translation. Psych. 5, e675.
Kumari, V., Antonova, E., Geyer, M.A., 2008. Prepulse inhibition and “psychosis-proneness” in healthy individuals: an fMRI study. Eur. Psychiatry 239 (23), 274–280.
Kumari, V., Gray, J., Geyer, M.A., Ffytche, D., Soni, W., Mitterschifftaler, M, 2003. Neural tactile prepulse inhibition: a functional MRI study in normal and schizophrenic subjects. Psychiatry Res. Neuroimaging 122, 99–113.
Lancaster, J.L., Woldorff, M.G., Parsons, L.M., Liotti, M., Freitas, C.S., Rainey, L., et al., 2000. Automated Talairach atlas labels for functional brain mapping. Hum. Brain Mapp. 10, 120–131.
Lei, M., Zhang, C., Li, L., 2018. Neural correlates of perceptual separation-induced enhancement of prepulse inhibition of startle in humans. Sci. Rep. 8, 472.
Li, L., Du, Y., Li, N., Wu, X., Wu, Y., 2009. Top-down modulation of prepulse inhibition of the startle reflex in humans and rats. Neurosci. Biobehav. Rev. 33, 1157–1167.
Li, X., Du, L., Sahlem, G.L., Badran, B.W., Henderson, S., George, M.S., 2017. Repetitive transcranial magnetic stimulation (rTMS) of the dorsolateral prefrontal cortex reduces resting-state insula activity and modulates functional connectivity of the orbitofrontal cortex in cigarette smokers. Drug Alcohol Depend 174, 98–105.
Liang, M., Mouraux, A., Iannetti, G.D., 2013. Bypassing primary sensory cortices–a direct thalamocortical pathway for transmitting salient sensory information. Cereb. Cortex 23, 1–11.
Logothetis, N.K., 2008. What we can do and what we cannot do with fMRI. Nature 453, 869–878.
Morgan, V.L., Dawant, B.M., Li, Y., Pickens, D.R., 2007. Comparison of fMRI statistical software packages and strategies for analysis of images containing random and stimulus-correlated motion. Comput. Med. Imaging Graph. 31, 436–446.
Neuner, I., Stocker, T., Kellermann, T., Ermer, V., Wegener, H.P., Eickhoff, S.B., et al., 2010. Electrophysiology meets fMRI: neural correlates of the startle reflex assessed by simultaneous EMG-fMRI data acquisition. Hum. Brain Mapp. 31, 1675–1685.
Palaniyappan, L., Simmonite, M., White, T.P., Liddle, E.B., Liddle, P.F., 2013. Neural primacy of the salience processing system in schizophrenia. Neuron 79, 814–828.
Richter, N., Warbrick, T., Mobascher, A., Brinkmeyer, J., Musso, F., Stoecker, T., et al., 2013. Epoch versus impulse models in the analysis of parametric fMRI studies. Clin. Neurophysiol. 124, 956–966.
Rissman, J., Gazzaley, A., D'Esposito, M., 2004. Measuring functional connectivity during distinct stages of a cognitive task. NeuroImage 23, 752–763.
Rohleder, C., Jung, F., Mertgens, H., Wiedermann, D., Sue, M., Neumaier, B., et al., 2014. Neural correlates of sensorimotor gating: a metabolic positron emission tomography study in awake rats. Front. Behav. Neurosci. 8, 178.
Rohleder, C., Wiedermann, D., Neumaier, B., Drzezga, A., Timmermann, L., Graf, R., 2016. The functional networks of prepulse inhibition:neuronal connectivity analysis based on FDG-PET in awake and unrestrained rats. Front. Behav. Neurosci 10, 148.
Röskam, S., Koch, M., 2006. Enhanced prepulse inhibition of startle using salient prepulses in rats. Int. J. Psychophysiol. 60 (1), 10–14.
Schell, A.M., Wynn, J.K., Dawson, M.E., Sinaii, N., Niebala, C.B., 2000. Automatic and controlled attentional processes in startle eyeblink modification: effects of habituation of the prepulse. Psychophysiology 37, 409–417.
Scholes, K.E., Martin-Iverson, M.T., 2009. Relationships between prepulse inhibition and cognition are mediated by attentional processes. Behav. Brain Res. 205, 456–467.
Scholes, K.E., Martin-Iverson, M.T., 2010. Disturbed prepulse inhibition in patients with schizophrenia is consequential to dysfunction of selective attention. Psychophysiology 47, 223–235.
Stein, T., Moritz, C., Quigley, M., Cordes, D., Haughton, V., Meyerand, E., 2000. Functional connectivity in the thalamus and hippocampus studied with functional MR imaging. AJNR 21, 1397–1401.
Swerdlow, N.R., Geyer, M.A., Braff, D.L., 2001. Neural circuit regulation of prepulse inhibition of startle in the rat: current knowledge and future challenges. Psychopharmacology (Berl) 156, 194–215.
Swerdlow, N.R., Weber, M., Qu, Y., Light, G.A., Braff, D.L., 2008. Realistic expectations of prepulse inhibition in translational models for schizophrenia research. Psychopharmacology (Berl) 199, 331–388.
Tabor, K.M., Smith, T.S., Brown, M., et al., 2018. Presynaptic inhibition selectively gates auditory transmission to the brainstem startle circuit. Curr. Biol. 28, 2527–2535.
Walter, A., Suenderhauf, C., Smieskova, R., Lenz, C., Harrisberger, F., Schmidt, A., et al., 2016. Altered insular function during aberrant salience processing in relation to the severity of psychotic symptoms. Front. Psychiatry 7, 189.
Wang, J.X., Rogers, L.M., Gross, E.Z., Ryals, A.J., Dokucu, M.E., Brandstatt, K.L., et al., 2014. Targeted enhancement of cortical-hippocampal brain networks and associative memory. Science 345, 1054–1057.
Whitfield-Gabrieli, S., Thermenos, H.W., Milanovic, S., Tsuang, M.T., Faraone, S.V., McCarley, et al., 2009. Hyperactivity and hyperconnectivity of the default network in schizophrenia and in first-degree relatives of persons with schizophrenia. Proc. Natl. Acad. Sci. USA 106, 1279–1284.
Wood, G., Nuerk, H.C., Sturm, D., Willmes, K., 2008. Using parametric regressors to disentangle properties of multi-feature processes. Behav. Brain Funct. 4, 38.
Wylie, K.P., Tregellas, J.R., 2010. The role of the insula in schizophrenia. Schizophren. Res. 123, 93–104.
Yang, N.B., Tian, Q., Fan, Y., Bo, Q.J., Zhang, L., Li, L., et al., 2017. Deficits of perceived spatial separation induced prepulse inhibition in patients with schizophrenia: relationships to symptoms and neurocognition. BMC Psychiatry 17, 135.
Zebardast, N., Crowley, M.J., Bloch, M.H., Mayes, L.C., Wyk, B.V., Leckman, J.F., et al., 2013. Brain mechanisms for prepulse inhibition in adults with Tourette syndrome: initial findings. Psych.Res. 214, 33–41.